ISSN 1063-7826, Semiconductors, 2008, Vol. 42, No. 5, pp. 580–588. © Pleiades Publishing, Ltd., 2008.
Original Russian Text © A.N. Razzhuvalov, S.N. Grinyaev, 2008, published in Fizika i Tekhnika Poluprovodnikov, 2008, Vol. 42, No. 5, pp. 595–603.

LOW-DIMENSIONAL SYSTEMS

# Hysteresis of Tunnel Current in *w*-GaN/AlGaN(0001) Double-Barrier Structures

**A. N. Razzhuvalov^ and S. N. Grinyaev^^**

*Kuznetsov Siberian Physicotechnical Institute, Tomsk State University, pl. Revolyutsii 1, Tomsk, 634050 Russia*

*^e-mail: shuvalov@phys.tsu.ru*

*^^e-mail: gsn@phys.tsu.ru*

Submitted June 5, 2007; accepted for publication October 17, 2007

**Abstract**—On the basis of a self-consistent solution of the Schrödinger and Poisson equations, the features of the tunnel-current hysteresis in *w*-GaN/AlGaN(0001) double-barrier structures are investigated. It is shown that the hysteresis loop depends on the mutual orientation of external and internal fields in the well and is wider at the voltage polarity when these fields compensate each other. Within the framework of the single-resonance approximation, a tunnel-current model in the double-barrier structure is developed, and the relation between the hysteresis-loop parameters and resonant states is found. It is established that the hysteresis loop can be relatively wide (~4 V) even in geometrically symmetric structures with the participation of two resonances. In asymmetrical structures, the change in the growth-surface type results in enhancement or suppression of the hysteresis loop depending on the alternation of nonequivalent barriers.

PACS numbers: 73.21.Fg, 73.63.Hs

**DOI:** 10.1134/S1063782608050163

## 1. INTRODUCTION

Nitride structures of *w*-GaN/AlGaN(0001) are used in various electronic devices, i.e., field-effect transistors, LEDs, lasers, photodetectors, switches, piezoelectric transducers, etc. [1]. They are promising for design of varactors [2], chemical sensors [3], etc. In recent years, interest in manufacturing resonance-tunneling diodes on their basis having pronounced characteristics with negative differential conductance (NDC) in a wide temperature range has continued to increase. The electron properties of nitrides are essentially modified by internal fields induced by spontaneous and piezoelectric polarizations. These fields lead to nonlinear features of the tunnel current: hysteresis, asymmetry, jumps, and bistability [4–12]. The majority of tunnel-current investigations are executed for the structures with the Ga (0001) growth surface having a higher quality of heteroboundaries, greater mobility, and higher density of two-dimensional electron gas in comparison with the materials with the N $(000\bar{1})$ growth surface [13].

The first resonance-tunnel diodes on the basis of *w*-GaN/AlN(0001) double-barrier and multiwell quantum structures with thin layers were reported in [4–8]. Asymmetrical behavior of the current with respect to altering the voltage polarity, a wide hysteresis loop (~6 V [7]), a large peak–valley ratio (~32) [8], the degradation of current peaks when switching the voltage [6, 7], and the dependence of characteristics on the growth conditions and the prehistory of the material were observed. The effect of various factors hampers the interpretation of the hysteresis, and its features remain a subject of discussion [7, 8].

The investigations of the tunnel current for the more studied GaAs/AlAs(001) double-barrier structures can serve to clarify this problem. The complex current–voltage (*I*–*V*) dependence (bistability and formation of a plateau in the hysteresis loop) in these structures was discovered for the first time in [14] and explained by the feedback effect for the electric field generated by electrons arriving to the well region on the tunnel current. The subsequent investigations of the time dependence of the tunnel current by the Wigner-function method [15] showed that the double hysteresis and current oscillations are related to the interaction of a resonance level in the main quantum well with the states of the triangular well arising in the spacer layer near the emitter barrier. The current hysteresis in these structures is observed at reasonably low temperatures, and the coercive force amounts to a relatively small value of ~0.05 V [15].

In the *w*-GaN/AlN wurtzite nitride structures, the hysteresis loop is more pronounced and observed at high temperatures up to room temperature due to a wide energy gap, large values of band and effective-mass discontinuities, and the effect of built-in fields. The tunneling processes in nitrides were simulated in [6, 9–12, 16, 17]. In [9], it is shown on the basis of the Green-function method that the diode character of the current is related to polarization charges at heteroboundaries, and qualitative agreement with the data [4] was obtained. However, this method renders it impossible to

explain the current hysteresis and bistability [6]. The causes of the discrepancies are associated with the electron traps modifying the interface-charge value [6] and the disregarded leakage current, the buffer-layer resistances, and the contact properties [10]. The tunnel current heavily depends on the spontaneous-polarization value. It has been shown [10] that the agreement with experiment is improved for a certain decrease in the polarization value determined by the Bury phase method [18]; this fact was confirmed in [19]. In AlGaN solid solutions, the surface charge decreases due to a nonlinear dependence on the spontaneous-polarization composition and the piezoelectric-tensor parameters [20].

Previously [12], on the basis of the joint solution of the Schrödinger and Poisson equations, we showed that the tunnel current of the $Al_{0.3}Ga_{0.7}N/GaN/Al_{0.3}Ga_{0.7}N$ double-barrier structure depends on the mutual orientation of internal and external fields in the well, and the structure's resistance is higher in the case where these fields compensate each other. The *I–V* characteristic of this structure is described well by the single-resonance model in which the electron tunneling is taken into account only via the lower resonance in the well.

In this study, we use this method for studying the features of the tunnel-current hysteresis arising with the involvement of one or two resonances. We consider the dependence of the tunnel current on the surface type of the grown structures.

## 2. COMPUTATIONAL METHOD

The *I–V* characteristics of the *w*-$GaN/Al_{0.3}Ga_{0.7}N(2c_1)/GaN(6c_2)/Al_{0.3}Ga_{0.7}N(2c_1)/GaN$ (0001) stressed geometrically symmetrical double-barrier structures ($c_1$ and $c_2$ are the lattice constant along the hexagonal axis) and those of the *w*-$GaN/Al_{0.3}Ga_{0.7}N(2c_1)/GaN(6c_2)/Al_{0.3}Ga_{0.7}N(3c_1)/GaN$ (0001) asymmetrical structures were investigated as in [12] on the basis of the self-consistent solution of the Schrödinger and Poisson equations. The quantum region of two barriers and wells was considered undoped, the GaN contact regions were heavily doped with silicon atoms (concentration $N_d = 5 \times 10^{19}$ cm$^{-3}$) with the ionization energy $E_d = 0.308$ eV. The electron states were described in the semiclassical approximation in the region of contacts adjoining the barriers and in the quantum ballistic approximation inside the double-barrier region. We disregarded the effect of the inelastic electron scattering by phonons on the electron charge, the structure effective potential, and the tunnel current. The internal fields induced by the spontaneous and piezoelectric polarization were taken into account within the framework of the macroscopic approach [17] in the quantum region. In the contact regions, these fields were considered to be compensated due to, for example, the free charges and the electron traps of the dislocation or defect states [6]. The tunnel-current density was calculated in the approximation of the isotropic effective mass via a difference in the electron fluxes impinging on the double-barrier region from the left- and right-hand sides [12]:

$$j = \frac{em^*kT}{2\pi^2\hbar^3}\int_{E_m}^{\infty} P(E) \times \left\{\ln\frac{1+\exp[(E_F - E)/kT]}{1+\exp[(E_F - eV - E)/kT]}\right\}dE, \quad (1)$$

where $E_m$ is the conduction-band-edge energy of the emitter at the boundary with the barrier, $e$ is the elementary charge, $m^*$ is the effective mass, $T$ is the temperature, $k$ is the Boltzmann constant, and $V$ is the voltage (it was assumed that the left-hand contact region is charged positively at $V > 0$ and that, in this case, the electrons move towards the left-hand contact). All energies are hereinafter counted from the conduction-band edge in the depth of the left-hand contact. Other details of the computational method for the transmission factor $P(E)$, the Fermi-level energy $E_F$, and the solutions of the Schrödinger and Poisson equations are given in [11, 12, 17].

For analyzing the nature of the current hysteresis loop, we calculated the bulk electron concentration $n(z)$ and surface electron concentration $n_w$ (in the GaN well), where the direction $z$ is perpendicular to heteroboundaries [12]: $n_w = \int_{well} n(z)dz$. Since the quantum region was assumed to be undoped and the inelastic-scattering processes were disregarded, the resonance level was taken to be unoccupied when it appeared below the conduction-band edge of the emitter.

## 3. TUNNEL CURRENT IN A SYMMETRICAL DOUBLE-BARRIER STRUCTURE

The calculated *I–V* characteristics of the *w*-$GaN/Al_{0.3}Ga_{0.7}N(2c_1)/GaN(6c_2)/Al_{0.3}Ga_{0.7}N(2c_1)/GaN$ symmetrical double-barrier structure (structure (262)) with the Ga growth surface at $T = 250$ K are shown in Fig. 1. The growth orientation ($z$) of this structure coincides with the polar axis [0001]. The density of the tunnel current $j$ and the concentration $n_w$ were determined for the continuous increase (forward portions, subscript *f*) and decrease (reverse portions, subscript *b*) of the voltage magnitude. In the structure with the N growth surface, the built-in fields in the layers are oppositely directed; therefore, the dependence $j(V)$ with the current and voltage signs opposite those in Fig. 1 correspond to this structure.

The pronounced NDC portion at $V < 0$, the jumps, and a wide hysteresis loop for the tunnel current at $V > 0$ are the features of the *I–V* characteristic. The analysis of the current density showed that its value is mainly related to the contribution of the electrons tunneling through the resonance level with the energy $E_r$ located

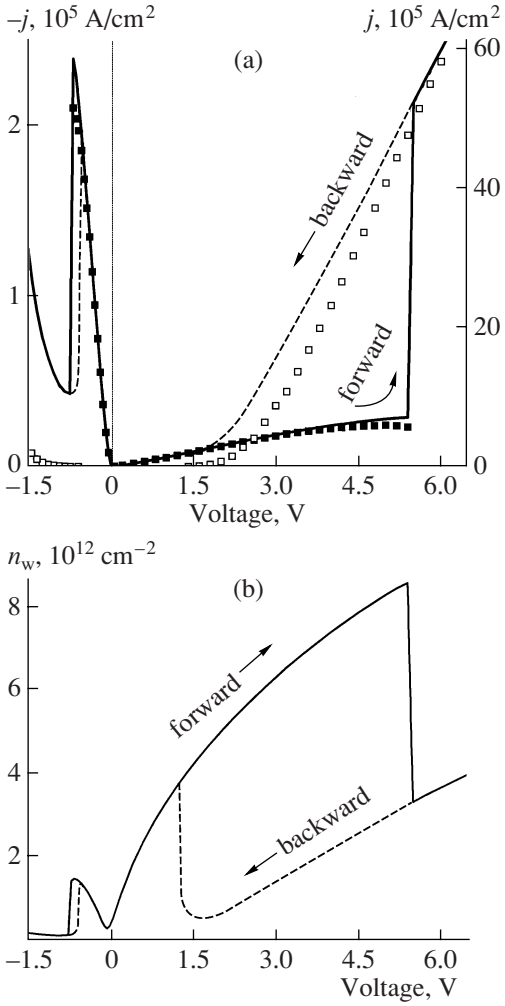


**Fig. 1.** (a) Tunnel-current density $j(V)$ and (b) the concentration $n_w$ of two-dimensional electron gas in the quantum well in the GaN/AlGaN($2c_1$)/GaN($6c_2$)/AlGaN($2c_1$)/GaN double-barrier structure at $T = 250$ K. Solid lines represent the forward portions from the exact calculation, and the dashed lines correspond to the reverse portions. (a): points represent the results of the "single-resonance" model calculation for the forward and reverse portions.

closest to the emitter quasi-Fermi level $E_F^{em}$ (equal to $E_F$ at $V < 0$ and $E_F - eV$ at $V > 0$). The current jumps are observed during the transition of the lower resonance level through the emitter conduction-band edge. The transitions occur in narrow intervals $V_{\lambda d}^{\pm} < V_{\lambda}^{\pm} < V_{\lambda u}^{\pm}$, $\lambda = (b, f)$ before (subscript $d$) and after (subscript $u$) critical negative (–) and positive (+) voltages $V_{\lambda}^{\pm}$. Within these intervals, the iterative procedure of the joint solution of the Schrödinger and Poisson equations is unstable. The current bistability similar to that observed in the GaAs/AlAs(001) structures [14, 21] can arise here. The stable solutions correspond to the interval edges, which are most close to $V_{\lambda}^{\pm}$. At $V < 0$, in which case the directions of external and internal fields in the well coincide, the curves of the current density have the NDC typical region with a narrow hysteresis loop: $-0.75\ \text{V} < V_f^- < -0.7\ \text{V}$ and $-0.60\ \text{V} < V_b^- < -0.55\ \text{V}$. At $V > 0$, the directions of external and internal fields in the well are opposite. In this case, we observed a large current-density jump in the voltage range of $5.4\ \text{V} < V_f^+ < 5.5\ \text{V}$, a small jump for $1.25\ \text{V} < V_b^+ < 1.30\ \text{V}$, a wide hysteresis loop (~4 eV), and extended portions of the linear dependence $j(V)$ at the forward and reverse branches.

The comparison between the dependences of the current density and the concentration $n_w(V)$ of 2D electron gas in a QW on the voltage shows that these dependences are similar: the increase (decrease) in the current density at the forward (reverse) branches corresponds to an increase (decrease) in the electron concentration in the well everywhere except the narrow regions near the critical voltages $V_{\lambda}^{\pm}$. For the voltage $V_f^+$, the current-density increase is accompanied by a decrease in the concentration; for the voltages $V_b^+$, $V_f^-$, and $V_b^-$, the current and concentration vary self-consistently.

The lowest concentration $n_w$ is shifted towards negative voltages to $V \approx -0.05$ V. This is related to the fact that, because of the asymmetry of the potential at low voltages, the $n_w$ value depends mainly on the electron flux from the direction of a less strong right-hand barrier, the contribution from which decreases with the growth of $|V|$ at $V < 0$ and increases at $V > 0$. At voltages $V < -0.05$ V, the concentration increases due to an increase in the flux from the direction of the left-hand barrier.

At critical voltages when the first resonance level falls below the edge or appears above the conduction-band edge of the emitter, the current jumps arise correspondingly at the forward or reverse portion of $j(V)$. In the case where this level (voltages $V_f^+$ and $V_f^-$) goes down, the electron charge and the potential energy $W$ in the well region decrease, and when this level appears (voltages $V_b^+$ and $V_b^-$), they increase. The voltage decrease after the $j(V)$ jump does not recover the $W$ profile to the $j(V)$ jump because of the difference in rates of the resonance-level and electron-concentration variation in the well with the voltage. However, the electron potentials, and with them the tunnel-current densities on the forward and reverse portions, coincide when the deepened resonance level again becomes available for the electron tunneling ($E_r > E_m$) at critical voltages $V_b^+$ and $V_b^-$. Due to the irreversible current of the electron-

charge redistribution at the current-jump moment, the hysteresis loop is formed.

Let us consider the tunnel-current features depending on the voltage polarity in more details.

*Positive voltages.* In the forward portion of $j(V)$, the potential of double-barrier structure becomes more and more symmetrical with increasing voltage, which enhances the wave-function localization and increases the electron charge in the well. This leads to the effect of negative feedback; i.e., the electron potential and the first resonance level $E_r$ are lowered with respect to the quasi-Fermi level $E_F^{em}$ with increasing voltage. However, this shift is largely compensated by the reverse shift associated with the charge accumulation in the well and the linear Stark effect arising due to the potential and probability-density asymmetry. Therefore, the level $E_r$ is close to $E_F^{em}$, but away from $E_m$ even in a large voltage interval. In agreement with the model [12], the $j(V)$ dependence is linear here. To the moment when the levels are equaled ($E_r = E_m$), such a large amount of charge is accumulated in the well that its outcome from the well after the first-resonance falling (Fig. 2a) induces a considerable lowering of the electron potential $W$ at which the second resonance level appears near $E_F^{em}$. As a result, the charge stabilizing the further potential drop is formed in the well again. Because the second peak of the transmission factor is much wider than the first peak, a large current jump arises at the voltage $V_f^+$. After the jump, the external and built-in fields inside the well almost completely compensate each other, and its bottom becomes flat. The electron density inside the well acquires the double-hump and almost symmetrical shape with the depleted region due to the $p$-like character of the second-resonance state, and the charge from this region outflows to the emitter region adjoining the quantum structure (inset in Fig. 2a) with the pronounced triangular shape of $W$. Due to a weak asymmetry in the probability density for the second resonance, the Stark effect is much more weakly pronounced for this resonance than for the first resonance.

As can be seen from Fig. 1, the reverse $I$–$V$ characteristic does not repeat the forward-portion trend at $V < V_f^+$ and is the continuation of its portion at $V > V_f^+$ retaining an almost linear form up to a voltage of ~3 V. Here, as well as at the forward portion, the negative-feedback effect also arises: the electron potential and the second resonance level are shifted upwards with respect to $E_F^{em}$ with decreasing voltage; however, this shift is in part compensated due to decreasing charge in the well. In this case, the second-level position is almost unaffected by the Stark effect. Because the charge in the well generated by the second resonance is much less than the

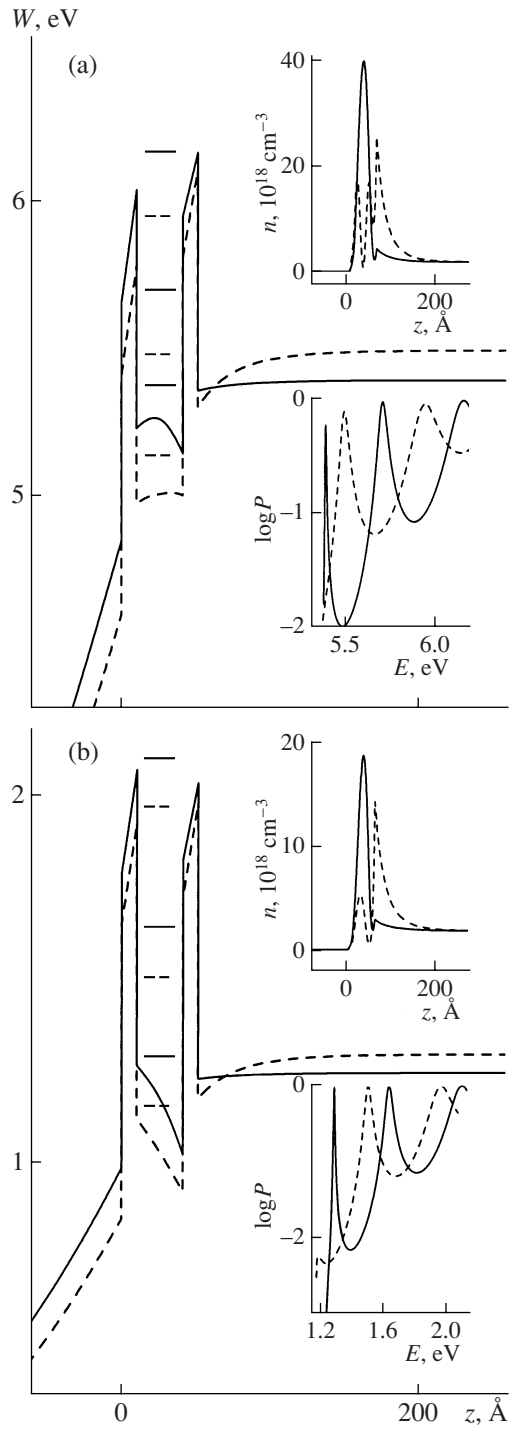


**Fig. 2.** Potential energy $W(z)$ in the GaN/AlGaN($2c_1$)/GaN($6c_2$)/AlGaN($2c_1$)/GaN double-barrier structure near the critical voltages (a) $V_f^+$ and (b) $V_b^+$: solid lines correspond to the voltages $V_{fd}^+ = 5.40$ V and $V_{bu}^+ = 1.25$ V, and the dashed lines correspond to $V_{fu}^+ = 5.50$ V and $V_{bd}^+ = 1.30$ V. In the insets, the corresponding transmission factors $P$ and the bulk electron concentrations $n$ are given. The position of resonance levels in the quantum wells is shown.

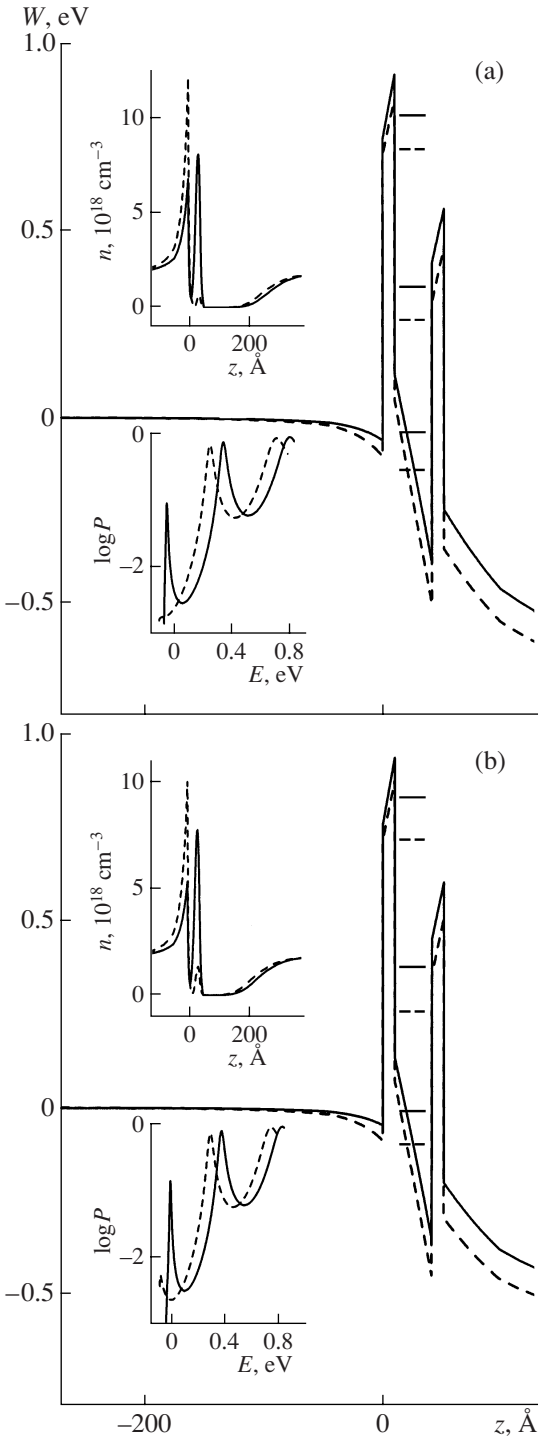


**Fig. 3.** Potential energy $W(z)$ in the GaN/AlGaN($2c_1$)/GaN($6c_2$)/AlGaN($2c_1$)/GaN double-barrier structure near the critical voltages (a) $V_f^-$ and (b) $V_b^-$: the solid lines correspond to the voltages $V_{fd}^- = -0.70$ V, $V_{bu}^- = -0.55$ V, and the dashed lines correspond to $V_{fu}^- = -0.75$ V and $V_{bd}^- = -0.60$ V. In the insets, the corresponding transmission factors $P$ and the bulk electron concentrations $n$ are given. The position of resonance levels in the quantum wells is shown.

corresponding charge generated by the first resonance, pinning of the second resonance level with respect to the quasi-Fermi level $E_F^{em}$ at the reverse portion appears much less rigid than that for the first resonance level at the forward portion. Achieving the voltage $V_b^+ = 1.3$ V, we observe a small increase in the current associated with opening the channel of tunneling via the first resonance level (Fig. 2b). After it, the current values at the forward and reverse portions coincide at $V < V_b^+$. The loop of the "double-resonance" hysteresis proved to be relatively wide, and $V_f^+ - V_b^+ \approx 4$ V due to the large difference of charges in the well and the rates of motion of resonance levels on the two current portions. Due to a small current jump at $V_b^+$, the loop width can be estimated from the intersection point of the linear portions of two characteristics.

*Negative voltages.* In this case, the directions of internal and external fields in the well coincide, and the current hysteresis is related to the involvement of only the lower resonance. With increasing $|V|$, the electron potential becomes more and more asymmetrical, and the resonance level is lowered according to the linear Stark effect [11]. Because of the small charge in the well, the effect of slowing down the level motion is weakly expressed; therefore, this level very quickly leaves the tunneling process for a relatively low critical voltage $V_f^- = -0.7$ V. In this case, because the potential jump proves to be smaller than the distances between the first and second resonance levels (Fig. 3), in contrast to the case $V > 0$, the tunnel current decreases (instead of increases) and forms the typical characteristic with the NDC. The further increase in the current at the forward portion with $|V|$ is caused by bringing the second resonance toward the $E_F^{em}$ level.

At the reverse portion at the critical voltage $V_b^- = -0.6$ V, the current experience jumps at the moment of opening the channel of tunneling through the first resonance. The voltages $V_f^-$ and $V_b^-$ are close to each other because of the small difference in potentials of the quantum region near the jump; therefore, the hysteresis loop at $V < 0$ proved to be narrow, $V_f^- - V_b^- \approx 0.1$ V.

## 4. TUNNEL-CURRENT MODEL FOR THE DOUBLE-BARRIER STRUCTURE

**A.** We clarify the causes of the difference in resistances on the forward and reverse current portions at $V > 0$. For this purpose, we use the "single-resonance" approximation [12] valid when the resonance level $E_r$ is close to the level $E_F^{em}$. In this case, the main contribution

to the tunnel current is given by a narrow transmission-factor range near $E_r$, which enables us to write $j$ as [12]

$$j = \frac{em^*kT}{4\pi\hbar^2}\frac{P_r}{\tau_r}\left\{\ln\frac{1+\exp[(E_F^{col}-E_r)/kT]}{1+\exp[(E_F^{em}-E_r)/kT]}\right\}\gamma_r, \quad (2)$$

where $P_r$ is the resonance transmission factor, $\tau_r$ is the resonance-state lifetime, $\Gamma_r = \hbar/\tau_r$ is the resonance-peak width,

$$\gamma_r = \frac{1}{2} + \frac{1}{\pi}\arctan\frac{E_r - E_m}{\Gamma_r/2},$$

and $E_F^{col}$ is the quasi-Fermi-level energy in the collector, equal to $E_F - eV$ at $V < 0$ and $E_F$ at $V > 0$. As can be seen from Fig. 1, the "single-resonance" approximation as a whole agrees well with the results of the exact calculation. A certain underestimation of the model current in the forward portions near $V_f^+$ and $V_f^-$ is related to the difference between "exact" $P(E)$ and the Lorentz shape used when deriving Eq. (2) [12]. At the reverse branch at $V > 0$, the discrepancy is larger in the region of low voltages because the contribution from the low-energy electrons removed from the resonance level in model (2) is incompletely taken into account. The considerable discrepancies are observed for voltages $V < V_f^-$ due to a small potential jump (~–0.1 eV); the second resonance here is appreciably removed from $E_F^{em}$.

For the voltages $|V| > 0.1$ V and the temperature $T =$ 250 K, the electron flux from the collector direction is negligible in comparison with the flux from the emitter direction. In this case, current density (2) is determined by three factors dependent also on the properties of the emitter resonant state. The first factor $N = \Gamma_r P_r$ characterizes the resonance-peak "power," and the structure conductance is proportional to it. The second factor ln(…) reflects the dependence of the current on the electron-state filling in the resonance region. In the third factor $\gamma_r$, the terms determine the "fraction" of participation of electrons with the energies in the region of the left-hand and right-hand shoulder of the tunnel-current resonance peak (we remind that the electrons with energies $E < E_m$ make no contribution to the current). In the case where the resonance level coincides with the $E_F^{em}$ level and is spaced to an interval exceeding the level half-width from $E_m$, tunnel current density (2) becomes $j_0 = \pm(em^*kT/4\pi\hbar^3)N\ln 2$ (we take the signs "+" at $V < 0$ and "–" at $V > 0$).

For the positive voltages in the ranges of 1.2 V $< V <$ 3.5 V on the forward branch and 3.2 V $< V <$ 4.4 V on the backward branch, the conditions $|E_F^{em} - E_r| \ll kT \ll$

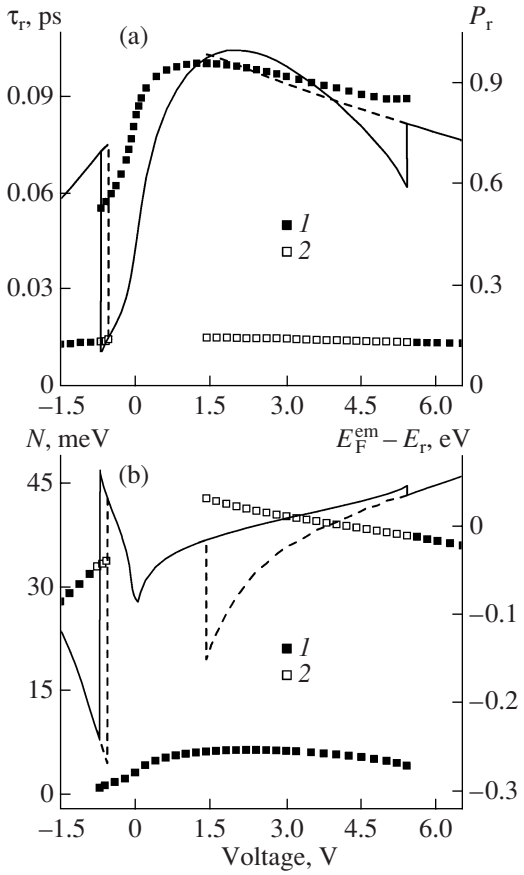


**Fig. 4.** Dependences of parameters of the "single-resonance" approximation on the voltage. The lines represent (a) the first-resonance lifetime $\tau_r$ and (b) the energy distance $E_F^{em} - E_r$ between the emitter quasi-Fermi level and the first-resonance level, the points correspond to (a) the transmission factor $P_r$ in the resonance and (b) the "power" $N$ of the first resonance peak. The solid curves and points *1* represent the forward sections, the dashed curves and points *2* represent the reverse portions.

$|E_F^{col} - E_r|, \Gamma_r/2 \ll |E_m - E_r|$, for which $\gamma_f^+ \approx 1$ and $\gamma_b^+ \approx 1$, are satisfied. This enables us to write the current density in the simplified form [12]

$$j = j_0 - \frac{em^*kT}{4\pi\hbar^3}N\left(\frac{E_F^{em} - E_r}{2kT}\right). \quad (3)$$

In the indicated regions, the resonance-level energies $E_{r\lambda}$ are almost proportional to the voltage, $E_F^{em} - E_{r\lambda} = \alpha_\lambda^+ + \beta_\lambda^+ V$ ($\lambda = f$, $\alpha_f^+ = -0.033$ eV, and $\beta_f^+ =$ 0.014 eV/V for the forward portion; $\lambda = b$, $\alpha_b^+ =$ –0.091 eV, and $\beta_b^+ = 0.024$ eV/V for the reverse portion). At the same time, the resonance-peak "strength" in these regions is virtually constant due to the corre-

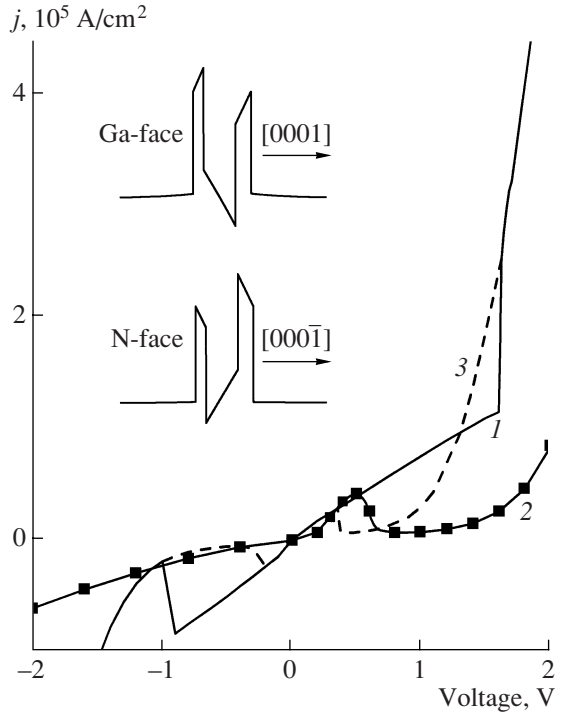


**Fig. 5.** *I–V* characteristics of the *w*-GaN/$Al_{0.3}Ga_{0.7}N(2c_1)$/GaN($6c_2$)/$Al_{0.3}Ga_{0.7}N(3c_1)$/GaN asymmetrical double-barrier structure with (*1*) the Ga growth surface and (*2*) the N growth surface. Curve (*3*) corresponds to the reverse portion. In the insets, the electron potentials are shown.

lated variation in $\tau_r$ and $P_r$ (Fig. 4); therefore, we can write the resistance of the double-barrier structure as

$$R_\lambda^+ = \frac{8\pi\hbar^3}{em^*S}\frac{1}{N_\lambda^+\beta_\lambda^+}, \quad (4)$$

where $S$ is the cross-section area. From Eq. (4), it follows that the ratio between the resistances on the forward and reverse portions of the tunnel-current hysteresis loop is

$$\frac{R_f^+}{R_b^+} = \frac{\tau_f^+}{\tau_b^+}\frac{P_b^+}{P_f^+}\frac{\beta_b^+}{\beta_f^+} = \frac{N_b^+\beta_b^+}{N_f^+\beta_f^+}. \quad (5)$$

In the middle of the linear portions of the forward ($V = 2.2$ V) and reverse ($V = 3.8$ V) segments, the ratios between parameters of two resonances (Fig. 4) are $\tau_f^+/\tau_b^+ = 7$, $P_b^+/P_f^+ = 0.9$, and $\beta_b^+/\beta_f^+ = 1.7$; therefore, the resistance at the forward portion proves to be approximately ten times higher than the resistances at the reverse portion. These ratios remain almost the same for other voltages in the indicated intervals; therefore, the difference in resistances at the forward and reverse portions is mainly related to the difference in the lifetimes of the first and second resonances.

**B.** We clarify the cause of the tunnel-current asymmetry at the linear segments of the forward portions between the critical voltages $V_f^+$ and $V_f^-$. The exact calculation of the resistances gives $R_f^+/R_f^- \approx 2.6$. The estimate of this ratio can be obtained using Eq. (3) for the tunnel current, which is applicable in the narrow interval $-0.4\text{ V} < V < -0.35$ V at the negative voltages. The resonance-peak "power" and the lower-level position in this interval linearly depend on the voltage, $N_f^- = \eta_f^- + \delta_f^- V$ ($\eta_f^- = 2.82$ meV, $\delta_f^- = 2.18$ meV/V), $E_F^{em} - E_{rf} = \alpha_f^- + \beta_f^- V$ ($\alpha_f^- = -0.049$ eV and $\beta_f^- = -0.151$ eV/V); therefore, the structure resistance becomes

$$R_f^- = \frac{8\pi\hbar^3}{em^*S}\frac{1}{\alpha_f^-\delta_f^- + \beta_f^-\eta_f^- + 2\beta_f^-\delta_f^-\bar{V}\gamma_f^-}\frac{1}{\gamma_f^-},$$

where $\bar{V} = -0.38$ V is the average voltage in the interval, and $\gamma_f^- \approx 0.89$. As a result, we obtain a ratio of resistances close to that in the exact calculation,

$$\frac{R_f^+}{R_f^-} = \frac{\bar{N}_f^-}{N_f^+}\frac{|\beta_f^-|}{\beta_f^+}\gamma_f^- = \frac{1.8\times 0.151}{6.6\times 0.014}\times 0.89 \approx 2.7,$$

where $\bar{N}_f^- = = \eta_f^- + \delta_f^-(\alpha_f^-/\beta_f^- + 2\bar{V})$ is the effective peak-power value taking into account the corrections on the square-law dependence on the model-current voltage. Hence, for the negative voltages, the resonance-level energy varies 11 times faster than for the positive voltages, whereas the peak "power" $\bar{N}_f^-$, on the contrary, is 4 times less than the peak "power" $N_f^+$. In Fig. 4, we show that these ratios approximately retain their values in a wider interval of negative voltages. Therefore, the tunnel-current asymmetry for the voltage-polarity alternation is caused mainly by the difference in the rates of resonance-level variation.

## 5. TUNNEL CURRENT IN ASYMMETRICAL DOUBLE-BARRIER STRUCTURES AND THE DEPENDENCE OF CURRENT ON GROWTH SURFACE

The results of calculation of the tunnel currents and potentials in the *w*-GaN/$Al_{0.3}Ga_{0.7}N(2c_1)$/GaN($6c_2$)/$Al_{0.3}Ga_{0.7}N(3c_1)$/GaN asymmetrical double-barrier structures (structures (263)) with the Ga and N growth surfaces are shown in Fig. 5. It should be taken into account when comparing them with the data for the symmetrical structure (262) (Fig. 1) that, due to the shift of the well-bottom potential (for the Ga surface, when the right-hand barrier is thicker, the well potential is shifted downwards relative to the well potential of the symmetrical structure (262), and the potential is shifted upwards for the N surface),

the resonance level of the structure (262) occupies the intermediate position (0.124 eV) between the resonance levels (0.104 and 0.153 eV) of the structures (263) with Ga and N surfaces, respectively.

The current-density jumps for the asymmetrical structure (262) with the Ga growth surface on the forward and reverse portions of $j(V)$ at critical voltages $V_f^+$ and $V_b^+$ are much smaller than in the case of the symmetrical structure (262). This is related to the fact that the resonance level is lowered with increasing the emitter-barrier thickness, and the rate of its variation increases with the voltage [11]. A decrease in the transparence of the asymmetrical structure (263) leads to an increase in its resistance. The critical voltage of the forward portion $V_f^-$ is increased insignificantly. However, due to the fact that a thicker collector barrier results in a greater localization of the wave function and in the accumulation of a greater charge in the well, the structure resistance increased essentially (almost threefold). After the resonance-level drop, the charge escapes from the well to the emitter region, and the potential is drastically lowered. Therefore, the critical voltage $V_b^- \approx -0.3$ V is much lower at the reverse portion than that in the structure (262). Such variations of $V_f^-$, $V_b^-$, $V_f^+$, and $V_b^-$ lead to an almost symmetrical shape and wide hysteresis loops for both voltage polarities of the tunnel current in the structure (263) with the Ga growth surface.

In the asymmetrical structure (263) with the N growth surface, the tunnel-current behavior is essentially different. At $V > 0$, a lone peak is observed at the voltage of 0.5 V, there is no hysteresis loop; at $V < 0$, the current jump occurs at a much higher voltage, $V_f^- \approx -7$ V (in Fig. 5, this jump and its allied hysteresis loop are not shown). To explain the differences, we note that the change in the order of barriers (263 $\longrightarrow$ 362) is equivalent to the change in the type of the structure surface and the polar-axis direction. For example, the potential profile of the *w*-GaN/$Al_{0.3}Ga_{0.7}N(3c_1)$/GaN($6c_2$)/$Al_{0.3}Ga_{0.7}N(2c_1)$/GaN structure with the Ga surface in the case of inversion with respect to the well center passes into that of the *w*-GaN/$Al_{0.3}Ga_{0.7}N(2c_1)$/GaN($6c_2$)/$Al_{0.3}Ga_{0.7}N(2c_1)$/GaN structure with the N surface within the shift equal to the barrier-thickness differences. Therefore, as in the case of the symmetrical structure (262), the dependences $j(V)$ for these structures at the same $z$-axis direction should differ only in sign if the difference in the morphology of two surfaces is disregarded.

The current peak for structure (263) with the N surface shifts towards lower voltages despite the fact that the resonance-level position in the quantum well is higher than that in the structure (262). This is explained by faster variation in this level energy relative to $E_F^{em}$ due to an increase in the emitter-barrier thickness [11] and weakening of the negative-feedback effect because of the fact that a smaller charge is accumulated in the well with a more asymmetrical potential. This was also the cause of the absence of the hysteresis loop at $V > 0$. At the negative voltages, the indicated factors favor an increase in the charge in the well that leads to an increase in the structure resistance and distancing the moment when the resonance level is equalized with the emitter quasi-Fermi level.

## 6. CONCLUSIONS

It is shown that a wide tunnel-current hysteresis loop appears in *w*-GaN/$Al_{0.3}Ga_{0.7}N$/GaN/$Al_{0.3}Ga_{0.7}N$/GaN(0001) double-barrier nitride structures at the voltages where the external and internal fields in the well are opposite each other. In this case, the structure potential becomes more and more symmetrical with the voltage increase, which leads to an increase in the electron charge in the well and to a profound negative-feedback effect manifesting itself in the slowed down approaching of the resonance level to the emitter quasi-Fermi level. This causes growth of the structure resistance and postpones the moment of the disappearance (fall) of the lower resonance from the tunneling process on the forward current portion. At the moment of fall, the population depletion of the resonant state takes place, and the charge escapes from the well to the emitter, which drastically lowers and deforms the active-region potential. In the GaN/$Al_{0.3}Ga_{0.7}N(2c_1)$/GaN($6c_2$)/$Al_{0.3}Ga_{0.7}N(2c_1)$/GaN (0001) symmetrical structure, the potential jump proved to be comparable with the energy gap between two resonance levels; therefore, the structure characteristics irreversibly switch to the second-resonance parameters at the critical voltage, while an increase in the structure transparence leads to a current jump. Upon voltage inversion, the potential does not recover its original shape and varies with the voltage faster due to a smaller charge in the well generated by the second *p*-type resonance. The decrease in the resistance at the reverse portion is mainly related to the decrease in the resonance-state lifetime. As a result, the first-resonance return voltage proves to be appreciably lower during the current transfer than the voltages of its withdrawal from this process, which leads to forming a wide hysteresis loop. The loop parameters are related to the characteristics of two resonances: peak powers of transmission factors, a charge value in the well, and the rate of motion of resonances with respect to the emitter Fermi level. The hysteresis-loop height is proportional to the variation in charge in the well during the transition of resonance from an open channel to the "dark" region and vise versa.

In GaN/$Al_{0.3}Ga_{0.7}N(2c_1)$/GaN($6c_2$)/$Al_{0.3}Ga_{0.7}N(3c_1)$/GaN(0001) asymmetrical double-barrier heterostructures, the change in the growth surface is not reduced to a simple tunnel-current inversion similar to the one that

takes place for the symmetrical structure (262) with ideal boundaries. This is related to the fact that the perturbation potential caused by internal fields changes the sign with the growth orientation and is asymmetrical with respect to the reflection in the plane passing through the well center. Therefore, the resonance-level position in the structures with Ga and N surfaces proves to be different and, along with it, the level-motion rate and the charge in the quantum well vary with the voltage. As a result, a drastic change in peak positions and peak-current values take place. For the considered structure (263), the transition from Ga to N growth surface results in the disappearance of the hysteresis loop when the directions of external and internal fields in the well coincide. Disregarding the morphological difference in Ga and N surfaces, the change in the growth surface is equivalent to that in the voltage polarity and barrier alternation.

## ACKNOWLEDGMENTS

We thank G.F. Karavaev for the useful discussion.

This study was supported by the Russian Foundation for Basic Research, project no. 06-02-16627-a and used the computing resources of the St. Petersburg branch of the Interdepartment Supercomputer Center.

## REFERENCES

1. S. C. Jain, M. Willander, J. Narayan, and R. Van Overstraeten, J. Appl. Phys. **87**, 965 (2000); O. Ambacher, M. Eickhoff, A. Link, et al., Phys. Status Solidi C **0**, 1878 (2003).
2. A. Reklaitis, Appl. Phys. Lett. **86**, 262110 (2005).
3. Y. Liu, M. Z. Kauser, D. D. Schroepfer, et al., J. Appl. Phys. **99**, 113706 (2006).
4. A. Kikuchi, R. Bannai, and K. Kishino, Phys. Status Solidi A **188**, 187 (2001).
5. A. Kikuchi and K. Kishino, Appl. Phys. Lett. **81**, 1729 (2002).
6. C. T. Foxon, S. V. Novikov, and A. E. Belyaev, Phys. Status Solidi C **0**, 2389 (2003).
7. A. E. Belyaev, C. T. Foxon, S. V. Novikov, and O. Makarovsky, Appl. Phys. Lett. **83**, 3626 (2003).
8. A. Kikuchi and K. Kishino, Appl. Phys. Lett. **83**, 3628 (2003).
9. K. M. Indlekofer, E. Donà, J. Malindretos, et al., Phys. Status Solidi B **234**, 769 (2002).
10. M. Hermann, E. Monroy, A. Helman, et al., Phys. Status Solidi C **1**, 2210 (2004).
11. S. N. Grinyaev and A. N. Razzhuvalov, Fiz. Tekh. Poluprovodn. **37**, 450 (2003) [Semiconductors **37**, 417 (2003)].
12. S. N. Grinyaev and A. N. Razzhuvalov, Fiz. Tekh. Poluprovodn. **40**, 695 (2006) [Semiconductors **40**, 675 (2006)].
13. O. Ambacher, J. Smart, J. R. Shealy, et al., J. Appl. Phys. **85**, 3222 (1999).
14. V. J. Goldman, D. C. Tsui, and J. E. Cunningham, Phys. Rev. Lett. **58**, 1256 (1987); V. J. Goldman, D. C. Tsui, and J. E. Cunningham, Phys. Rev. B **35**, 9387 (1987); A. Zaslavsky, V. J. Goldman, D. C. Tsui, and J. E. Cunningham, Appl. Phys. Lett. **53**, 1408 (1988).
15. P. Zhao, H. L. Cui, D. Woolard, et al., J. Appl. Phys. **87**, 1337 (2000).
16. F. Sacconi, A. DiCarlo, and P. Lugli, Phys. Status Solidi A **190**, 295 (2002).
17. S. N. Grinyaev and A. N. Razzhuvalov, Fiz. Tverd. Tela **43**, 529 (2001) [Phys. Solid State **43**, 549 (2001)].
18. F. Bernardini, V. Fiorentini, and D. Vanderbilt, Phys. Rev. B **56**, R10024 (1997).
19. J. Simon, R. Langer, A. Barski, and N. T. Pelekanos, Phys. Rev. B **61**, 7211 (2000).
20. V. Fiorentini, F. Bernardini, and O. Ambacher, Appl. Phys. Lett. **80**, 1204 (2002).
21. P. Zhao, H. L. Cui, and D. L. Woolard, Phys. Rev. B **63**, 075302 (2001).

*Translated by V. Bukhanov*